EUKARYOTIC CELL, Dec. 2007, p. 2354–2364 Vol. 6, No. 12
1535-9778/07/$08.00+0 doi:10.1128/EC.00128-07

Kinesin-13 Regulates Flagellar, Interphase, and Mitotic Microtubule Dynamics in *Giardia intestinalis*▽†

Scott C. Dawson,[1,2]* Meredith S. Sagolla,[1] Joel J. Mancuso,[1] David J. Woessner,[2] Susan A. House,[2] Lillian Fritz-Laylin,[1] and W. Zacheus Cande[1]

Department of Molecular and Cell Biology, University of California–Berkeley, 341 LSA Bldg., Berkeley, California 94720,[1] and Section of Microbiology, 255 Briggs Hall, University of California–Davis, Davis, California 95616[2]

Received 17 April 2007/Accepted 18 July 2007

Microtubule depolymerization dynamics in the spindle are regulated by kinesin-13, a nonprocessive kinesin motor protein that depolymerizes microtubules at the plus and minus ends. Here we show that a single kinesin-13 homolog regulates flagellar length dynamics, as well as other interphase and mitotic dynamics in *Giardia intestinalis*, a widespread parasitic diplomonad protist. Both green fluorescent protein-tagged kinesin-13 and EB1 (a plus-end tracking protein) localize to the plus ends of mitotic and interphase microtubules, including a novel localization to the eight flagellar tips, cytoplasmic anterior axonemes, and the median body. The ectopic expression of a kinesin-13 (S280N) rigor mutant construct caused significant elongation of the eight flagella with significant decreases in the median body volume and resulted in mitotic defects. Notably, drugs that disrupt normal interphase and mitotic microtubule dynamics also affected flagellar length in *Giardia*. Our study extends recent work on interphase and mitotic kinesin-13 functioning in metazoans to include a role in regulating flagellar length dynamics. We suggest that kinesin-13 universally regulates both mitotic and interphase microtubule dynamics in diverse microbial eukaryotes and propose that axonemal microtubules are subject to the same regulation of microtubule dynamics as other dynamic microtubule arrays. Finally, the present study represents the first use of a dominant-negative strategy to disrupt normal protein function in *Giardia* and provides important insights into giardial microtubule dynamics with relevance to the development of antigiardial compounds that target critical functions of kinesins in the giardial life cycle.

Giardia intestinalis is the most frequently identified protozoan cause of intestinal morbidity worldwide (59) and has a two-stage life cycle: a "trophozoite," or flagellate, form that attaches to the intestinal microvilli and a cyst form that can persist in the environment (1, 21). As in other eukaryotes, the giardial microtubule cytoskeleton creates a stable scaffold for intracellular trafficking, for organelle attachment, and for cell polarization (21). However, other important functions of the microtubule cytoskeleton are dynamic and rely upon both intrinsic dynamic instability—stochastic switches between microtubule growth and shrinkage phases (43)—and active regulation of microtubule assembly and/or disassembly. Microtubule dynamics, for example, are critical during cell division in *Giardia* where the two nuclei (30) undergo mitosis with extranuclear spindles that penetrate at polar nuclear openings (58), followed by the duplication and repositioning of eight flagella into the daughter cells (75). Beyond descriptions of cytoskeletal movements, we currently have little understanding of the molecular mechanism of active regulation of interphase and mitotic microtubule dynamics in *Giardia*.

One class of conserved regulators of microtubule dynamics that mediate interactions between microtubule plus ends and other organelles are the plus-end tracking proteins (+TIPs). +TIPs include both microtubule-associated proteins such as EB1 and CLIP-170 (2) and kinesin motors such as kinesin-13 and kinesin-8 homologs (25, 77). +TIPs track to the polymerizing ends of microtubules (44) and regulate microtubule dynamics in vivo (13). Beyond interphase function, most +TIPs are also associated with kinetochores during mitosis (2), presumably to facilitate the search and capture of chromosomes by microtubules to ensure proper chromosome segregation. Microtubule +TIPs such as EB1 and several kinesin motors (kinesin-13 and kinesin-8) direct both mitotic and interphase microtubule dynamics in metazoans (25, 42, 44, 77).

Microtubule depolymerization dynamics in the spindle are regulated by kinesin-13 (reviewed recently in reference 45), a nonprocessive motor protein with an internal motor domain. Kinesin-13 is targeted to microtubule plus ends by lattice diffusion (28) and forms rings around microtubules (71), where it promotes depolymerization (10). Members of the kinesin-13 family (such as MCAK [for mitotic centromere-associated kinesin]) have important roles in regulating microtubule dynamics in mitotic arrays, particularly in the establishment of proper kinetochore-microtubule attachments and mitotic progression (33, 42, 79). Beyond mitotic functions, two *Drosophila* kinesin-13 homologs have been shown to promote microtubule depolymerization in interphase arrays (33, 42). In *Drosophila*, a specific interaction between EB1 and kinesin-13 has been observed wherein the EB1 homolog recruits the kinesin-13 homolog, KLP10A, to interphase microtubule plus ends (42). Kinesin-13 homologs are present in the sequenced genomes of many flagellated eukaryotes (7, 54, 80), and yet are absent in some nonflagellated organisms, such as budding and fission yeast (80).

* Corresponding author. Mailing address: Section of Microbiology, University of California–Davis, 255 Briggs Hall, One Shields Ave., Davis, CA 95616. Phone: (530) 752-3633. Fax: (530) 752-9014. E-mail: scdawson@ucdavis.edu.

† Supplemental material for this article may be found at http://ec.asm.org/.

▽ Published ahead of print on 31 August 2007.

Giardia has a sole kinesin-13 homolog, and our aim here was to understand its function in both interphase and mitosis using a kinesin-13 (S280N) rigor mutant that resulted in a dominant-negative phenotype. By adapting a methodology that has been used to create kinesin mutants in other organisms (23, 36), we generated an inducible ectopic rigor kinesin-13 mutant, the first use of such an approach to generate cytoskeletal mutants in vivo in *Giardia*. We found that the rigor kinesin-13 mutant resulted in a dominant-negative phenotype that affected not only spindle microtubule dynamics but also flagellar length. Flagellar motility is critical for the completion of *Giardia*'s life cycle in the mammalian host both during interphase and during late stages of cytokinesis. In particular, flagellar motility is required for *Giardia* to find suitable sites to attach and detach from the surfaces including the intestinal villi (12). The recent report that kinesin-13 also regulates flagellar length in *Leishmania* suggests that active regulation of microtubule depolymerization at the flagellar tip by kinesin-13 may be a widespread and evolutionarily conserved mechanism important for flagellar-length determination in many organisms (7). We also determined that kinesin-13 also has a novel function in regulating microtubule dynamics in the "median body," a unique giardial microtubule organelle of undetermined function. This study of kinesin-13 function in *Giardia* underscores the universality of kinesin-13-mediated regulation of microtubule dynamics in both interphase and mitotic cytoskeletal arrays, including both arrays unique to *Giardia* and common arrays (such as axonemes and spindles) found in most other eukaryotes.

MATERIALS AND METHODS

Strains and culture conditions. *G. intestinalis* trophozoites, strain WBC6 (ATCC 50803), were maintained at 37°C in modified TYI-S-33 medium with bovine bile (31) in either 13-ml screw-cap tubes (Fisher) or on coverslips in eight-well dishes (Fisher) placed in BioBags (Fisher) to maintain a low-oxygen environment. For the analysis of spindles, mitotic cells were enriched (10 to 20% on average) by growing 1 to 2 days past confluence and then adding fresh, warmed medium and collecting cells for analysis at 1-h intervals over a 3- to 7-h period.

Cloning and transformation of GFP-tagged EB1, kinesin-13, and kinesin-13 (S280N) rigor mutant strains. We modified pGFPa.pac (64) by ligating complementary oligonucleotides (MCSA [5′-AGCTTGGCGCGCCGATATCCGGAT-3′] and MCSB [5′-ACCGCGCGGCTATAGGCCTATCGA-3′]) into the HindIII restriction site for making green fluorescent protein (GFP) fusions. Both the kinesin-13 and the EB1 homologs were amplified from *G. intestinalis* strain WBC6 (ATCC 50803) genomic DNA using PCR (including ~80 bp upstream of the start codon to include the native promoter, and AscI/AgeI sites were for subcloning) with the oligonucleotide primer pair K13aF (5′-GGCGCGCCAAG ACACTGTCTCCTCTTACCAATTTACTC-3′ and K13aR (5′-ACCGGTAGT TTCTTCCTGGCCTTATTGAGGTCTATGGAATGGCTG-3′) and the primer pair EB1F (5′-GGCGCGCCTGTGTCTTGCATGCGTGAGCTAAGTTGGG TAGAAACGTAAGT-3′) and EB1R (5′-ACCGGTGGATCCGGCAGTATCT GATGATACTCCGCATACAGAATATC-3′). To create a GFP-tagged, tetracycline-repressible kinesin-13 (S280N) rigor construct, a giardial episomal vector with a tetracycline-repressible promoter (70) was modified to replace the luciferase gene with an eGFP sequence by PCR amplification from the pGFPa.pac vector using the oligonucleotide primers: GFPTETF (5′-ACTAGTCCCTATC AGTGATAGAGAGGCGCGCCTAGGATCCACCGGTACCGGTCCTCAT GGTGAGCAAGGGCGAGGA-3′) and GFPTETR (5′-CTGCAGAGGATGG ACCAACGCCGTTGGAAGAAGGAAAACCACTAACCATTGAGGCCCA GGAA-3′). The eGFP amplicon was then ligated into a SpeI/PstI digest of the episomal vector (70) to create the tetracycline-inducible GFP fusion vector pTetGFPC.pac. By adapting a methodology that has been used to create kinesin mutants in other organisms (23, 36), we generated an inducible ectopic kinesin-13 (S280N) rigor mutant in *Giardia*. To create the inducible kinesin-13 (S280N) rigor mutant construct, the kinesin-13 homolog was PCR amplified from *Giardia* genomic DNA (using TK13F [5′- GGCGCGCCATGTCTGACT TGGTTTACCAGTGGCTCGAGTCAGC-3′] and TK13R [5′-ACCGGTAGTT TCTTCCTGGCCTTATTGAGGTCTATGGAATGG-3′]) and cloned downstream of the *ran* promoter and associated tetO elements in pTetGFPC.pac. The kinesin-13 ATP rigor mutation (S280N) construct was designed based on a multiple sequence alignment of kinesin-13 homologs from diverse eukaryotes and was constructed by site-directed mutagenesis (Stratagene QuikChange site-directed mutagenesis kit) of the previous construct using the oligonucleotide primers (k13DNF [5′-GGACAAACTGGCTCGGGGAAAAATTTCACTATG ATG] and k13DNR [5′-CATCATAGTGAAATTTTTCCCCGAGCCAGTTTG TCC]); the point mutation was confirmed by DNA sequencing.

***G. intestinalis* strain.** WBC6 was transformed by electroporation with roughly 50 μg of plasmid DNA using a GenePulserXL (Bio-Rad) as previously described (16), with the following modifications: 375 V, 1,000 μF, and 25 Ω. Episomes were maintained by antibiotic selection in transformants using 50 μg of puromycin (Calbiochem)/ml (16). Tet-mediated repression of the kinesin-13 (S280N) rigor mutant constructs was maintained with 10 μg of doxycycline (Sigma)/ml prior to induction experiments.

QPCR analysis of kinesin-13 (S280N) overexpression. Total cellular RNA was isolated from 6-ml cultures from both uninduced and induced kinesin-13 (S280N) rigor mutant strains at 15 and 30 min, as well as 1, 8, 16, 24, and 48 h after induction using a Cells-to-cDNA kit (Ambion). For quantitative analysis of expression 1-μl aliquots of the cDNA synthesis were used in subsequent actin (actF [5′-CCTGAGGCCCCCGTGAATGTGGTGG-3′] and actR [5′-GCCTCT GCGGCTCCTCCGGAGG-3′])- and GFP (GFPF [5′-GAGCTGTTCACCGG GGTGGTGCCC-3′] and GFPR [5′-CGGGCATGGCGGACTTGAAGAAGT CGTGC-3′])-specific PCR amplifications in the DyNamo HS SYBR green pPCR master mix (Finnzymes). Quantitative PCR was performed with an Opticon 2 system (Bio-Rad). Control cDNA syntheses that lacked reverse transcriptase were also performed with original RNA extractions to demonstrate that RNA samples were not contaminated with DNA. GFP overexpression was compared by using the relative method of quantification (37), and GFP expression levels were normalized to the actin gene. Overexpression was determined from comparisons of normalized GFP expression in induced time points to uninduced controls.

Immunofluorescence microscopy and image data analysis. For GFP fixation, trophozoites were incubated in HEPES-buffered saline for 20 min prior to fixation in 1% paraformaldehyde for 30 min at 37°C. For experiments with the kinesin-13 (S280N) rigor mutant strain, tetracycline (doxycycline) repression was removed for 48 h prior to immunostaining. After fixation, cells were centrifuged (1,500 × *g* for 5 min), washed three times in 1× PEM (100 mM PIPES, 1 mM EGTA, 0.1 mM $MgSO_4$), and attached to poly-L-lysine-coated coverslips (1 mg/ml). Cells were permeabilized in 0.1% Triton X-100 for 10 min, washed in PEM, and blocked for 30 min in PEMBALG (PEM plus 1% bovine serum albumin, 0.1% sodium azide, 100 mM lysine, and 0.5% cold water fish skin gelatin). To visualize microtubules, we incubated the coverslips at room temperature with TAT1, a monoclonal antibody to α-tubulin (81) (directly labeled with a Xenon fragment conjugated to an Alexa 555 fluorophore [Molecular Probes, Eugene, OR]) at a 1:75 dilution. Coverslips were washed three times in PEMBALG and PEM and mounted and counterstained with DAPI (4′,6′-diamidino-2-phenylindole) using ProLong AntiFade (Molecular Probes).

Images were collected with DeltaVision image acquisition software SoftWoRx (Applied Precision) by using an Olympus IX70 wide-field inverted fluorescence microscope with an Olympus UPlanApo 100X, NA 1.35, oil immersion objective lens and a Photometrics charge-coupled device CH350 camera cooled to −35°C (Roper Scientific). Serial sections were acquired at 0.2-μm intervals and were deconvolved by using the SoftWoRx deconvolution software. For presentation purposes, two-dimensional projections were created from the three-dimensional data sets using SoftWorX. Flagellar length measurements (based on immunostaining of axonemes for Taxol and nocodazole experiments) were calculated from three-dimensional image stacks by using SoftWorX image analysis tools. Median body volume measurements were made using the Imaris (BitPlane) software package.

TEM of flagellar tips, scanning electron microscopy (SEM), and flagellar length measurements. To determine the ultrastructure of the distal flagellar tips, trophozoites were prepared for transmission electron microscopy (TEM) first attached to sapphire discs and then were high-pressure frozen as described previously but with a few adjustments (60). Briefly, cells were allowed to attach to clean sapphire discs while being incubated at 37°C. Discs with attached cells were dipped into 20% bovine serum albumin in culture medium before they were placed into the specimen holder. Cells were frozen by using a Baltech high-pressure freezer and freeze substituted using a Leica freeze substitution apparatus. Discs with cells were embedded with Epon resin and

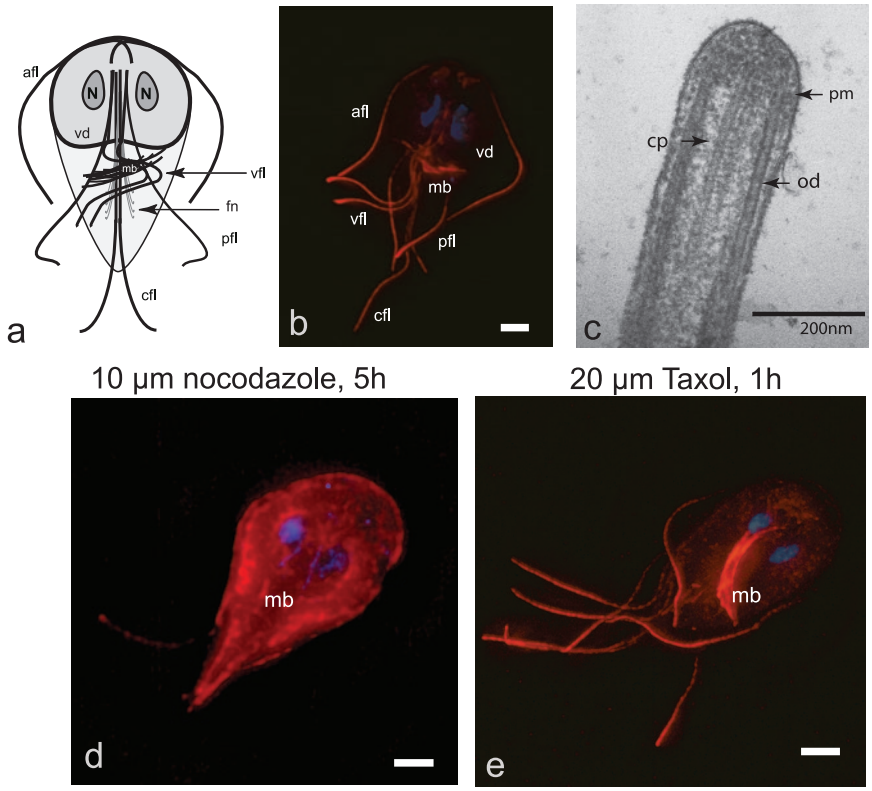

FIG. 1. The lengths of the axonemes, median bodies, and spindles are dynamic and sensitive to nocodazole and Taxol. (a) The giardial microtubule cytoskeleton is defined by four main structures: eight flagellar axonemes (caudal [cfl], anterior [afl], posterolateral [pfl], and ventral [vfl]), the ventral adhesive disc (vd), the funis (fn), and the median body (mb) (21) are diagrammed. (b) Anti-tubulin immunostaining illustrates the long cytoplasmic portions of axonemes compared to external membrane-bound regions and are presented as two-dimensional projections of three-dimensional stacks. (c) Ultrastructure at the distal flagellar tip of a caudal flagellum (cp, central pair; od, outer doublet; pm, plasma membrane). (d) In interphase after treatment with 10 μM nocodazole for 5 h, all eight axonemes (afl, cfl, vfl, and pfl [see panel a]) showed statistically significant depolymerization (see Table 1). The size and presence of the median body (mb) is also dramatically reduced after the addition of nocodazole. The diffuse staining of the cell body (due to unpolymerized tubulin subunits) and increased tubulin staining at the distal tips (due to accumulation of unpolymerized tubulin subunits) is increased in nocodazole-treated cells. (e) Additionally, both the median body (mb) and all eight axonemes increased in length significantly after Taxol stabilization of microtubules (see also Table 1). Scale bars, 2 μm.

serial sectioned on a Ultracut E. Sections were stained with uranyl acetate in 70% methanol and lead citrate and viewed with a JEOL 1200 transmission electron microscope.

For SEM, trophozoites were first allowed to attach to either to Aclar or track membrane filters and subsequently fixed for 1 h in 2% glutaraldehyde in cacodylate buffer. The cells were then postfixed with 2% OsO_4, dehydrated in ethanol, critically pointed dried, and coated with the MED 020 Bal-Tec high-vacuum coating system using iridium. Images were taken by using a Hitachi S5000 FESEM at 10 Kv.

Nocodazole and Taxol treatments. To determine the sensitivity of cytoskeletal arrays to microtubule depolymerizing and microtubule stabilizing compounds, we treated trophozoites with either nocodazole or Taxol for several hours prior to immunostaining and measurements of axonemal lengths. Specifically, nocodazole (Sigma, St. Louis, MO) was added at a final concentration of 10 μM to trophozoites, which were then incubated at 37°C for 5 h, prior immunostaining. Taxol (Paclitaxel; Sigma, St. Louis, MO) was added at a final concentration of 20 μM to trophozoites for 1 h at 37°C.

Nucleotide sequence accession numbers. The sequences of the *Giardia* kinesin-13 and EB1 homologs have been deposited in the GenBank database with the accession numbers DQ395239 and DQ395240, respectively.

RESULTS

Microtubule stabilization and destabilization drugs highlight dynamic microtubule arrays. *Giardia* has several major interphase cytoskeletal arrays: the median body, the ventral disc, the funis, and eight axonemes that possess both cytoplasmic and membrane-bound regions (Fig. 1a and b; see also reference 21). Each of the eight axonemes has a canonical 9+2 ultrastructure throughout the length of the flagellum, including the distinctive long cytoplasmic regions. The ultrastructure of the distal flagellar tips, however, has not been previously characterized. To determine whether there was any unique ultrastructure at the distal flagellar tip, we used TEM to image the caudal axonemes (Fig. 1c). *Giardia* axonemes had the canonical flagellar ultrastructure of a motile flagellum, and each axoneme contained conserved structures such as the central pair apparatus. There was no obvious cap structure linking the central pair and outer doublet axonemal microtubules to the flagellar membrane, as has been reported in *Chlamydomonas* (19). Finally, *Giardia* has two mitotic spindles that are responsible for chromosome segregation via canonical kinetochore microtubule attachments (17, 58), despite prior claims that *Giardia* has a spindle-independent mode of karyokinesis (4, 69).

We have previously shown that short (15-min to 1-h) incu-

TABLE 1. Axoneme length is dynamic and is significantly affected by nocodazole or Taxol treatment

Treatment group	Mean length (μm) ± SD[a]	
	Anterior	Caudal
Untreated	11.55 ± 1.20 (24)	6.26 ± 1.51 (23)
Nocodazole treated	9.11 ± 1.55 (31)*	3.72 ± 2.01 (34)*
Taxol treated	15.20 ± 1.61 (32)*	10.23 ± 1.58 (31)*

[a] Both anterior and caudal flagellar lengths were measured from the cell body to the distal tip as described in Materials and Methods. Mean lengths of the anterior axonemes and the standard deviation of the mean are reported, followed by the total number of axonemes in parentheses. Treatment with nocodazole resulted in ca. 22% shorter anterior (−2.44 μm) or 41% shorter caudal (−2.52 μm) axonemes compared to untreated controls. Treatment with Taxol resulted in ca. 30% longer anterior (+3.65 μm) or 60% longer caudal (+3.97 μm) axonemes compared to untreated controls. Asterisks denote highly statistically significant (as determined by using a two-tailed Student *t* test with unequal variances) anterior or caudal axoneme length differences after treatment of trophozoites with 10 μM nocodazole or 20 μM Taxol compared to untreated controls.

bations with the microtubule drugs Taxol and nocodazole affect microtubule dynamics in dividing cells resulting in broken spindles and various chromosome segregation defects (58). To determine the variation in microtubule dynamics in the giardial interphase microtubule arrays, we tested the effect of short (1 h, i.e., fewer than one cell cycle) incubations of drugs (Fig. 1d and e and Table 1), which have been shown to effect microtubule dynamics in other eukaryotes. Our assays are distinct from other studies in *Giardia* that used long incubation periods of 24 to 72 h, wherein after these long incubations dead cells are prevalent (38).

Flagella in other flagellated protists are generally insensitive to microtubule stabilizing or destabilizing drugs (20, 72). In *Giardia*, however, we found that trophozoites incubated in 10 μM nocodazole for 5 h showed a significant decrease in external flagellar length of all eight flagella of ca. 20 to 40% (Fig. 1d and Table 1). We also observed a dramatic shortening of microtubules in the median body (Fig. 1d). We have previously observed a dramatic effect of nocodazole on the dual mitotic spindles using the same experimental conditions (58).

Conversely, we used the microtubule-stabilizing drug Taxol to determine whether microtubule stabilization would lengthen dynamic microtubule arrays (Fig. 1e). After incubation with Taxol for less than one cell cycle, we found that all eight axonemes and the median body increased in length. Specifically, after the stabilization of interphase microtubules with 20 μM Taxol for 1 h, the average length of axonemes increased by 30 to 60% (Fig. 1e and Table 1) and that of the median body increased by roughly 42%. Although the ventral disc microtubules are not stained very intensely by the tubulin antibody used in the present study, disc morphology was not noticeably distorted by either drug treatment.

Both +TIPs EB1 and kinesin-13 localize to dynamic microtubule structures, including the distal tips of axonemes. To investigate the possible regulators of microtubule dynamics in *Giardia*, we focused our efforts on +TIPs, including EB1 and kinesin-13. EB1 is an evolutionarily conserved +TIP that is hypothesized to have diverse and possibly overlapping cellular activities: mediating the delivery of proteins to the cell periphery, modulating microtubule dynamics, and/or participating in the search and capture function of microtubules. EB1 has been studied extensively in metazoans (5, 11, 73), plants (41, 76), fungi (74), and *Chlamydomonas* (49, 65), but a conserved function of EB1 in marking polymerizing microtubule plus ends has not been demonstrated in *Giardia*. The use of GFP-tagged proteins has facilitated the study of +TIPs such as EB1, CLIP-170, and kinesin-13 (63). Therefore, we generated a C-terminal EB1:GFP fusion, using the sole giardial EB1 homolog (see Materials and Methods). We observed that in *Giardia*, the EB1:GFP fusion localized to the same arrays that are affected by compounds that disrupt microtubule dynamics, including the median body (Fig. 2) and the mitotic spindles (data not shown). EB1:GFP was particularly enriched at the distal tips of axonemes and axonemal exit points (or flagellar pores [21]). However, EB1:GFP localization was absent from the ventral disc. Thus, the EB1:GFP fusion localized to the same arrays that are affected by compounds that disrupt microtubule dynamics (Fig. 1), including the median body (Fig. 2).

In a survey of GFP-tagged kinesins, we classified (see Fig. S1 in the supplemental material) and localized a giardial kinesin-13:GFP fusion to the distal tips of axonemes, to the cytoplasmic anterior axonemes, to the median body (Fig. 3a to c), and to the mitotic spindles (Fig. 3d to f). As seen with the GFP-tagged EB1 (Fig. 2), kinesin-13:GFP localized to the same cytoskeletal elements most affected by microtubule stabilizing and destabilizing drugs: the distal tips of axonemes, the median body, and kinetochores of the mitotic spindles (Fig. 1d and e).

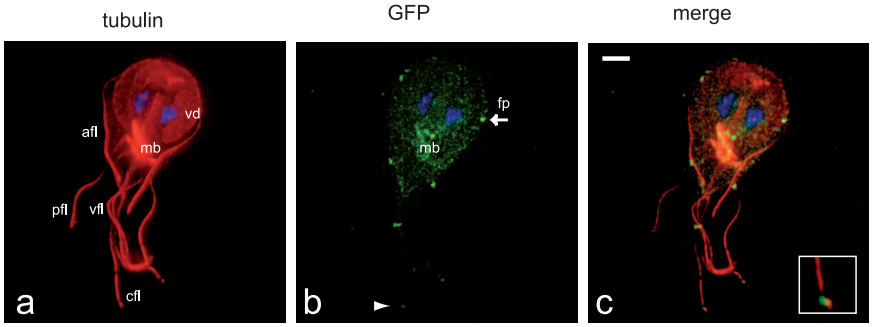

FIG. 2. The plus end-tracking protein EB1 localizes to all flagellar tips, the median body, and the mitotic spindles. The giardial EB1:GFP fusion localized to the distal flagellar tips (indicated by arrowheads), the median body (mb), the flagellar pores (fp, indicated by arrow), and the mitotic spindles (data not shown). (a) Tubulin; (b) GFP; (c) Merged image. Scale bar, 2 μm.

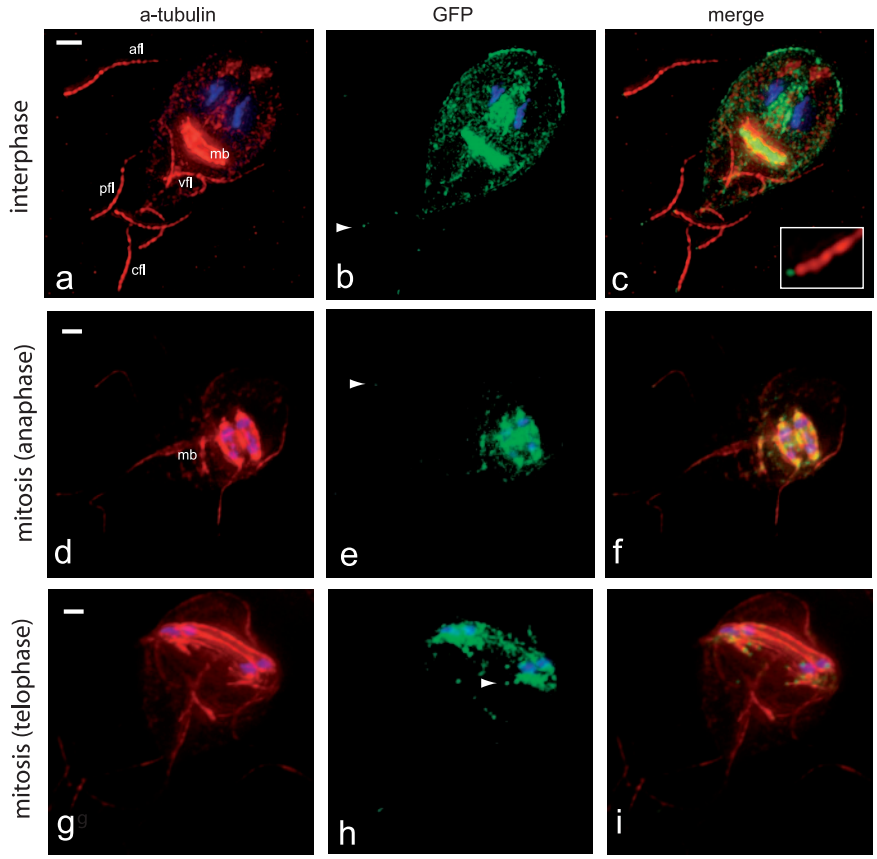

FIG. 3. Kinesin-13 localizes to flagellar tips, the median body, and mitotic spindles. (a to c) The kinesin-13:GFP fusion localized primarily to the distal flagellar tips (indicated by arrowheads) and the median body (mb). Some GFP staining was also observed at cytoplasmic regions of axonemes (primarily the anterior axonemes [afl]), but not to flagellar pores. Kinesin-13:GFP also localizes to the plus ends of microtubules and kinetochores in anaphase spindles (see also Fig. S2 in the supplemental material). Flagellar growth is initiated during anaphase and completed during the early stages of cytokinesis. During flagellar duplication kinesin-13:GFP localizes to the growing flagellar tips (arrowheads) of the posterolateral (pfl) and ventral (vfl) axonemes and to kinetochores (g to i). The flagellar lengths of both kinesin-13:GFP and EB1:GFP are unaffected by the presence of the GFP tag, and the decrease in axoneme length in both strains after nocodazole-treatment is similar to that of untreated controls (see Fig. S3 and Table S1 in the supplemental material).

In addition, kinesin-13 is associated with the either the intracellular axonemes of the anterior or ventral flagella (22). In nocodazole-treated kinesin-13:GFP cells, we found that flagellar length was reduced to an extent similar to that in wild type and that kinesin-13 localization was unaffected (see Fig. S3 and Table S1 in the supplemental material). Kinesin-13 also localizes to growing flagellar tips during mitotic telophase—particularly to the two axonemal pairs (the posterolateral [pfl] and ventral ([fl] pairs) that form de novo during giardial cell division (48) (Fig. 3g to i).

In vivo induction of a kinesin-13 rigor mutant results in a dominant-negative phenotype in both interphase and mitosis. To determine the role of the giardial kinesin-13 homolog in the regulation of microtubule disassembly in diverse microtubule arrays, we constructed a strain expressing a tetracycline-repressible GFP-tagged, rigor mutant kinesin-13 (S280N) (see Materials and Methods and Fig. 4). This particular point mutation is based on prior precedent of mutations in the kinesin ATPase domain, which permits binding of ATP but prevents its hydrolysis, and it has been used successfully in many other experimental systems to disrupt kinesin function (8, 10, 23, 32). The GFP tag allowed us to identify and characterize the cytoskeletal phenotypes of ~1-fold overexpression of the rigor mutant (see Fig. S4 in the supplemental material).

At 48 h after the removal of tetracycline repression, we observed dramatic changes in axonemal length, median body volume (Fig. 4d to f, Fig. 6d to f, and Table 2), and chromosome segregation defects compared to the same strain under repression (Fig. 4a to c and Fig. 6a to c). After induction of the kinesin-13 rigor mutant, we quantified axoneme length by using either SEM or immunostaining of the microtubule cytoskeleton and found that caudal flagellar length from the exit point to the tip increased in a statistically significant manner (>270% or +7 μm) relative to flagellar length in uninduced controls (Fig. 4 and 5 and Table 2). Median bodies with significantly (~42%) smaller volumes also resulted from the induction of the rigor kinesin-13 (S280N) mutant (Fig. 6d to f and Table 2) compared to the uninduced control (Fig. 6a to c). In early mitosis in the induced rigor mutant, the median body increased dramatically in length (Fig. 4g to i) and persisted throughout mitosis into cytokinesis, resulting in severe cytokinesis defects (Fig. 6g to i).

During mitosis, kinesin-13:GFP and the rigor mutant kinesin-13:GFP (S280N) have a similar distribution and localize to

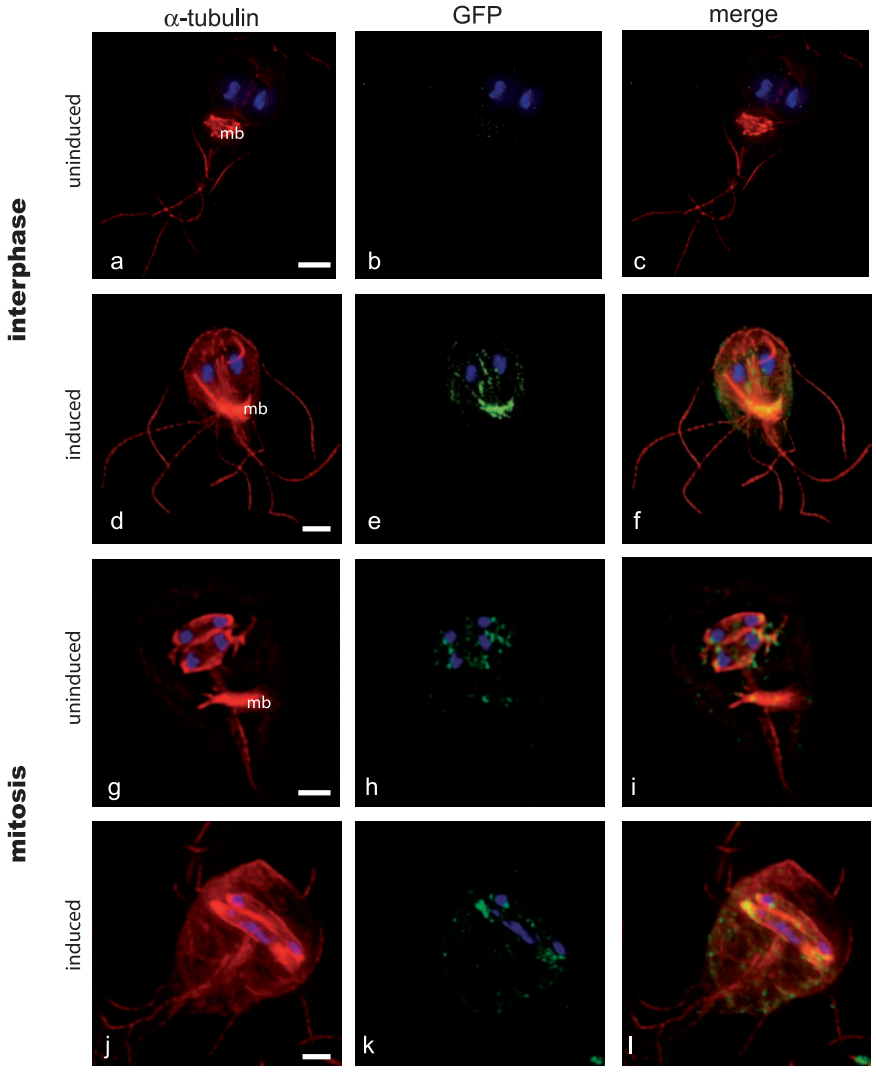

FIG. 4. Kinesin-13 promotes active disassembly of axonemes, spindles, and the median body. To test the function of kinesin-13, we created a kinesin-13 (rigor) mutant (S280N) under the control of a tetracycline-repressible promoter (see Materials and Methods). This strain had a dominant-negative phenotype and was immunostained with anti-alpha-tubulin to visualize and quantify external axoneme length (from the cell body to distal tip) following induction of the dominant-negative construct. The expression of the kinesin-13 (S280N) rigor mutant resulted in significantly longer flagella (d to f) compared to the uninduced control (a to c; see also Fig. 5). Additional phenotypes of the rigor mutant included cell division defects (see Fig. S3 in the supplemental material). During mitosis, induction of the kinesin-13 (S280N) rigor resulted in defective spindle function (j to l), as indicated by a high proportion of lagging chromosomes in ~80% of induced cells compared to uninduced controls (g to i). Scale bars, 2 μm.

TABLE 2. Median body volume is dynamic and significantly reduced after induction of the rigor mutant kinesin-13 (S280N)

Cell group	Avg ± SD[a]		
	Median body vol (μm^3)	Cell vol (μm^3)	Median body vol/ cell vol ratio
Uninduced	16.80 ± 6.34 (10)	253.91 ± 85.83 (10)	0.07 ± 0.02* (10)
Induced for 48 h	8.13 ± 6.68 (12)	185.13 ± 46.34 (12)	0.04 ± 0.02* (12)

[a] Median body volume (μm^3) was measured as described in Materials and Methods for both induced and uninduced cells (using the same cells measured for axoneme length). The average total cell volumes, average median body volumes, and ratios of median body volume to normalized total cell volume are reported. We also report the standard deviations of the mean, followed by the total number of cells measured in parentheses. Median body volumes decrease by ca. 42% by 48 h postinduction of the kinesin-13 (S280N) episomal construct. Asterisks denote highly statistically significant median body volume differences (as determined by using a two-tailed Student *t* test with unequal variances).

single spots on chromosomes (Fig. 4g to l), a distribution identical to that previously reported for the centromeric histone cenH3 (17). Further, we observed similar spindle defects, including lagging anaphase chromosomes (Fig. 4g to l), in mitotic cells of the rigor mutant kinesin-13 strain, as has been observed in diverse eukaryotes (79). This result is consistent with the hypothesis that kinesin-13 is localized to the giardial kinetochore and plays a role in anaphase A chromosome-to-pole movements.

DISCUSSION

Giardia cytoskeletal biology has both clinical and nonclinical relevance in terms of parasitology, cell biology, and evolution

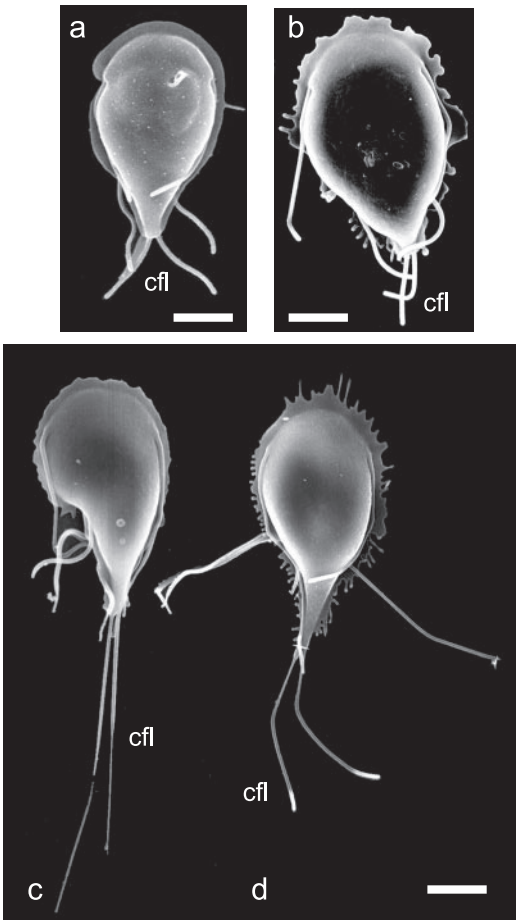

FIG. 5. SEM and quantification of elongated axonemes after induction of the kinesin-13 (S280N) rigor mutant. After induction of the kinesin-13 (S280N) construct, we used SEM to analyze both cell shape and flagellar length. Panels c and d show the dramatic elongation of flagellar axonemes (particularly the caudal [cfl] axonemes) compared to wild type (a) or uninduced cells (b). Note the aberrations at the distal tips of axonemes (d) (thickened or stretched compared to the wild type). Flagellar lengths were measured from the cell body to the distal tip after 48 h of induction of the kinesin-13 (S280N) construct. Induction resulted in statistically significant length elongation ($P < 0.001$) of all flagella, including caudal flagella (11.17 ± 1.62 μm, $n = 62$) by ~270% compared to uninduced controls (4.12 ± 1.44 μm, $n = 20$). Anterior, posterolateral, and ventral flagella were also significantly elongated by ca. 100% after 48 h of induction of the kinesin-13 (S280N) rigor mutant construct (data not shown).

(21). The interphase microtubule cytoskeleton in *Giardia* (see Fig. 1a and b) consists of both unique structures (the median body and the ventral disc) and more conserved structures (eight axonemes and two mitotic spindles). In particular, the "ventral disc"—a spiral microtubule array—is critical to virulence by mediating the attachment of trophozoites to the intestinal microvilli (21). The contribution of microtubule dynamics to the functioning of the these arrays (see Fig. 1) has not been previously established. In the present study, we have determined that the sole giardial kinesin-13 homolog regulates both interphase and mitotic microtubule disassembly dynamics in the eight distal flagellar tips, the median body, and the dual mitotic spindles.

Identification of dynamic microtubule arrays in *Giardia*. To determine the pattern and extent of interphase microtubule dynamics in *Giardia*, we first used both microtubule stabilization and destabilization drugs—commonly used to demonstrate the dynamic properties of the mitotic spindle (29)—to affect the complex interphase microtubule arrays in *Giardia* (Fig. 1d and e). While many microtubule arrays, including flagellar axonemes, were affected by drugs, there was no discernible effect on the ventral disc. Although it is difficult to visualize ventral disc microtubules due to accessibility problems, the faintly stained disc was not noticeably altered in morphology. Moreover, neither GFP-tagged EB1 nor kinesin-13 are found in the ventral disc, suggesting that this microtubule array may be more stable than the other drug-sensitive interphase arrays that contain these proteins.

Since axonemes in metazoans and *Chlamydomonas* are insensitive to microtubule destabilizing drugs, intrinsic microtubule dynamics may play a more important role in giardial axonemal length determination than in other flagellated protists. We propose that nocodazole affects the length of axonemes by sequestering tubulin subunits, thereby inhibiting intraflagellar transport (IFT)-mediated assembly of external axonemes. This shifts the dynamic equilibrium in favor of axonemal disassembly and results in shortened flagella (Fig. 1d). In a similar way, nocodazole treatment disrupts the equilibrium microtubule dynamics in the median body, since the sequestration of tubulin subunits results in small median bodies (Fig. 1).

In contrast, Taxol stabilization of microtubules shifted the dynamic equilibrium in favor of IFT-mediated axonemal assembly, resulting in the observed length increases (Table 1). Previously, Mariante et al. (38) had reported severe cytoskeletal defects in *Giardia* after treatment with 10 μM nocodazole for over 24 h (two to four cell cycles) but did not investigate effects on interphase microtubule dynamics at intervals shorter than 24 h. By using shorter incubation intervals with both Taxol and nocodazole that do not extend past one cell cycle, we observed a significant effect on the interphase microtubule dynamics of all eight axonemes, as well as the median body (Fig. 1d and e and Table 1) in contrast to the findings of Mariante et al. (38).

Ultrastructure at the distal tips of giardial flagella. The ultrastructure of the eukaryotic motile flagella is conserved among evolutionarily diverse eukaryotic microbes (47, 52, 66), with few exceptions (53, 62). *G. intestinalis* has a somewhat unique flagellar organization, however, in that all eight axonemes possess long cytoplasmic regions before exiting at the flagellar pores (reviewed recently in reference 21). Our TEM analyses clearly show that the ultrastructure of the axonemes retain the canonical 9+2 arrangement of doublet microtubules but appear to be missing a flagellar tip complex. Since axonemes in metazoans and *Chlamydomonas* are comparatively less sensitive to microtubule stabilizing and destabilizing drugs, intrinsic microtubule dynamics may have a more pronounced contribution to flagellar-length determination in *Giardia* than in many other organisms. This could possibly be due to differences in the ultrastructure of the flagellar tips (Fig. 1c and see Fig. S5 in the supplemental material), namely, the apparent absence of the flagellar tip complex.

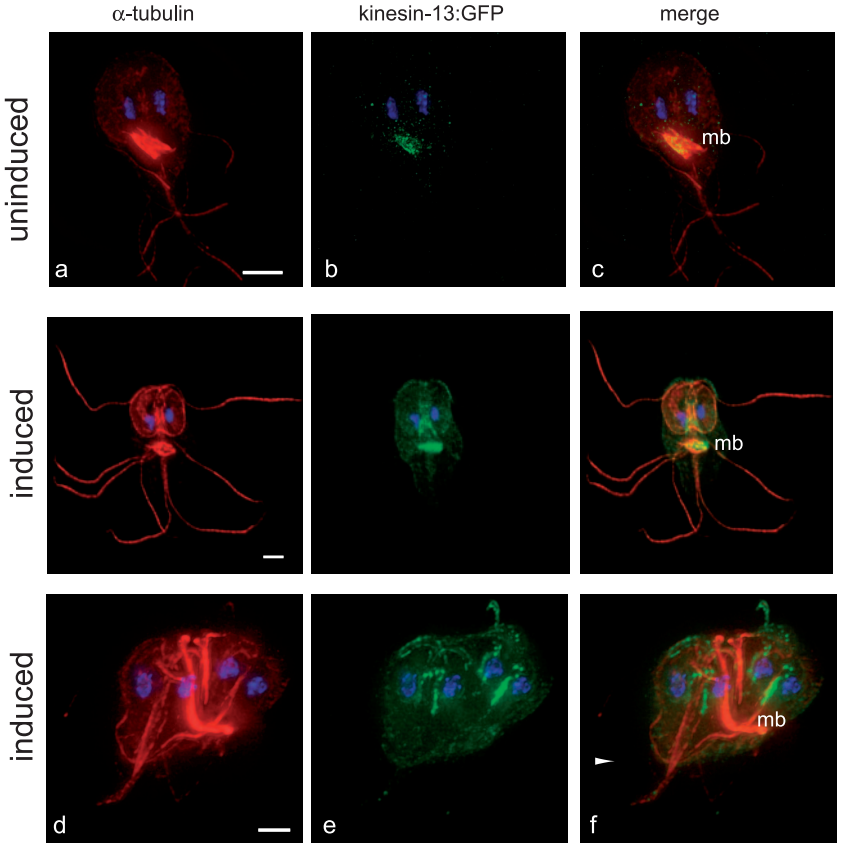

FIG. 6. Induction of the kinesin-13 (S280N) rigor mutant results in a dramatic elongation of the median body and cell division defects. Both uninduced and induced strains were immunostained with anti-alpha-tubulin to visualize the microtubule cytoskeleton after induction of the kinesin-13 (S280N) rigor mutant construct. In addition to effects on flagellar length and chromosome segregation (Fig. 4), the induction of the kinesin-13 (S280N) rigor mutant also resulted in cell division defects, including incomplete cytokinesis and incorrect positioning of the median body (d to f). Note the accumulation of kinesin-13:GFP staining at the distal flagellar tips (arrow). Scale bars, 2 μm.

EB1, a +TIP, localizes to microtubule plus ends in the dynamic giardial microtubule arrays. The effect of both Taxol and nocodazole on interphase microtubule dynamics in *Giardia*, particularly on of the axonemes, suggested that microtubule dynamics are important in maintaining flagellar length. To determine whether any active regulators of microtubule dynamics are present in *Giardia*, we looked at the localization GFP-tagged EB1 and kinesin-13, both proteins known to localize to actively polymerizing microtubule plus ends.

The giardial EB1:GFP localization suggests that it has a conserved function in regulating microtubule assembly at microtubule plus ends, including the distal flagellar tips (49). In interphase, the disruption of EB1 in both yeasts and vertebrates results in short microtubules (reviewed in reference 2). Thus, EB1 is thought to promote microtubule polymerization by either increasing the frequencies of rescue from catastrophic microtubule depolymerization or decreasing the rates of microtubule depolymerization (27, 35).

In *Chlamydomonas*, EB1, as well as IFT proteins and microtubule motors, accumulates both at the flagellar tips and at the flagellar basal bodies (49, 78). The basal body/transition zone region has thus been suggested as a docking site for the organization of IFT particles, based on such immunolocalization of kinesin-2 homologs and IFT proteins to basal bodies (18) and the disruption of basal body localization in either kinesin-2 mutants (15, 78) or KAP mutants (46). Several mechanisms for EB1 function in *Chlamydomonas* have been suggested, including recruiting proteins to the distal flagellar tip, promoting dynamic instability, or mediating the transition from anterograde to retrograde IFT (50). We observed EB1 localization to the flagellar pores, which suggests that IFT rafts do not dock at the basal bodies but rather at flagellar pores for transport along the membrane-bound portion of the axoneme. It is likely that EB1 could mediate the transition from anterograde to retrograde IFT in *Giardia*, since it localizes to both the flagellar exit point and the distal flagellar tips (Fig. 2).

Kinesin-13 is an active regulator of flagellar-length dynamics. Growth and maintenance of flagellar length is dependent upon IFT to provide building blocks to the site of assembly, the distal flagellar tip (34). IFT was initially discovered in *Chlamydomonas* (34) and has been well studied in experimental systems such as *Chlamydomonas* and *Caenorhabditis elegans* (reviewed in references 57and 61). Recent phylogenomic surveys indicate that IFT components are conserved across diverse parasitic protists, including *Giardia* (9). In terms of flagellar growth and assembly, both IFT proteins and the heterotrimeric kinesin-2 complex are present and have conserved functions in the flagellar assembly of external regions of axonemes in

Giardia (S. C. Dawson et al. unpublished data); based on both kinesin-13:GFP localization to the distal flagellar tips and the dramatic increases in flagellar length in the kinesin-13 rigor mutant strain, we suggest that kinesin-13 regulates flagellar length in all giardial axonemes through the promotion of microtubule disassembly (55). The relevance of this observation toward understanding regulation of flagellar length in other organisms is supported by the demonstration by Blaineau et al. that overexpression or knockdown of kinesin-13 expression in *Leishmania* alters flagellar length (7).

What are the relative contributions of inherent dynamic instability, IFT-mediated assembly, and kinesin-13-mediated microtubule disassembly to maintaining equilibrium axoneme length? The "balance point model" of flagellar length control postulates that axonemal length is maintained by equilibrium between length-dependent rates of assembly and length-independent rates of disassembly (39, 40). Active microtubule depolymerization by kinesin-13 at the distal axonemal tip would act as a mechanism to promote microtubule disassembly and turnover of tubulin subunits. Our analysis of kinesin-13 function in giardial axoneme length suggests that hierarchical levels of flagellar-length regulation (see Fig. S5 in the supplemental material), involving intrinsic microtubule dynamics and active assembly (by IFT and possibly EB1) and microtubule disassembly (by kinesin-13). Thus, the kinesin-13 dominant-negative resulted in flagellar elongation by continued flagellar assembly with decreased microtubule disassembly. The observed axonemal disassembly after nocodazole treatment (Fig. 1d) was due to limiting IFT-mediated assembly and active (kinesin-13-mediated) disassembly.

We propose that EB1 functions either to facilitate microtubule plus-end recognition by other +TIPs, such as kinesin-13 or, alternatively, aids in the localization of kinesin-13 to the microtubule plus ends at the distal flagellar tips (see Fig. S5 in the supplemental material). Kinesin-13, however, is able to translocate to microtubule plus or minus ends in the absence of EB1 in vitro (28). Changes in flagellar length dynamics presumably do not affect the cellular distribution of either EB1 or kinesin-13. In nocodazole-treated giardial trophozoites, both EB1 and kinesin-13 remained localized to the flagellar tips (see Fig. S3 and Table S1 in the supplemental material).

Kinesin-13 regulates microtubule dynamics in the median body. The median body is a semiorganized microtubule array found only in *G. intestinalis* and close relatives (see Fig. 1a and b) (21). Although proposed functions of the median body include either serving as a reservoir of microtubules or somehow functioning in cell division (51), there has been no experimental analysis of its function. Because both kinesin-13:GFP and EB1:GFP localized to the median body, we suggest that it is a dynamic structure with actively regulated microtubule plus ends. Kinesin-13 could play a role in median body disassembly during mitosis to liberate stores of tubulin for spindle or flagellar assembly. At 48 h after the induction of the dominant-negative kinesin-13 (S280N) construct, we observed a 42% reduction in median body volume (Table 2 and Fig. 6). Thus, while flagella elongated by roughly 3-fold, median bodies decreased in volume by approximately two-fifths, a finding consistent with the notion that the median body acts as a reservoir of microtubules in the cell (and similar to nocodazole-treated cells [Fig. 1d]). Further investigation of median body dynamics in live cells is required to confirm this hypothesis, however. In addition, the expression of the kinesin-13 rigor construct resulted in cells with a distorted interphase cell shape (Fig. 5c), suggesting that microtubule dynamics of the median body also influences giardial cell shape.

Kinesin-13 retains an evolutionarily conserved function in the regulation of spindle dynamics in the semi-open mitosis in *Giardia*. *Giardia* has a semi-open mitosis with two extranuclear spindles that access chromatin through polar openings in the nuclear membranes. In many eukaryotes, the metaphase mitotic spindle maintains a constant length, and +TIPs that modulate MT dynamics are the major governors of spindle length dynamics (2). Previously, we have shown that mitotic spindle length and structure in *Giardia* is affected by both nocodazole and Taxol as in other eukaryotes (26, 67; S. C. Dawson et al., unpublished data). Here we demonstrate a conserved mitotic localization of kinesin-13 at kinetochores of the dual giardial spindles (Fig. 3d to i and see Fig. S3 in the supplemental material). Further, through the analysis of mitotic cells in the in the kinesin-13:GFP (S280N) strain (Fig. 4g to l), we found a high number of cells (>50%) with visible mitotic defects, including spindle defects and lagging anaphase chromosomes (Fig. 4g to l). This phenotype of the kinesin-13 dominant-negative mutant on the structure of mitotic spindles has been observed in many diverse eukaryotes (79). However, this is the first demonstration of kinesin-13 function in mitosis in an organism with a semi-open mitosis (spindle poles external to the nuclear envelope (58) and kinetochore microtubules that penetrate the nuclei at polar openings (58). We suggest that the role of kinesin-13 at kinetochores and in the maintenance of spindle length is analogous to that in metazoans (24). This interpretation is supported by our preliminary observation that, as in metazoan spindles (73), EB1 is also found at giardial kinetochores (data not shown).

What are the ancestral functions of kinesin-13? Studies of the giardial cytoskeleton provide a unique evolutionary and comparative perspective to cytoskeletal mechanisms in other well-studied experimental systems. *Giardia* has been proposed to be a member of the earliest branches in single or multigene eukaryotic phylogenies when an archaeal outgroup is included (6, 14, 68). Although somewhat controversial in terms of its basal phylogenetic position, *Giardia* remains perhaps the most divergent eukaryote whose microtubule dynamics have been studied.

Giardia has fewer paralogs of cytoskeletal proteins (including kinesin-13) that have resulted from recent gene duplications, unlike metazoans (three kinesin-13 homologs) and trypanosomes (six kinesin-13 homologs) (see Fig. S1 in the supplemental material). Kinesin-13 homologs are present in multiple copies in phylogenetically diverse eukaryotes, and these multiple kinesin-13 homologs have been shown to cooperatively regulate interphase and mitotic microtubule dynamics (42). However, one would imagine that the ancestral eukaryote cell possessed only a single kinesin-13 that had multiple functions, analogous to the single giardial kinesin-13.

Both flagellar ultrastructure and the structural and regulatory molecular components of flagellar axonemes and microtubule plus ends are conserved in *Giardia*. We propose that the role kinesin-13 plays in giardial cytoplasmic and mitotic microtubules and in flagellar length dynamics is, in fact, an ancient

function and is therefore highly conserved in the evolution of the eukaryotic cell. Thus, the universal roles and regulation of kinesin-13 in giardial microtubule dynamics could extend to both novel and conserved microtubule-based structures (such as axonemes) in other more commonly studied eukaryotes.

ACKNOWLEDGMENTS

We thank Heidi Elmendorf and Steve Singer (Georgetown University); C. C. Wang and coworkers (University of California at San Francisco); and Keith Gull (University of Manchester, Manchester, United Kingdom) for plasmids, reagents, and methodologies. We especially thank Olivier Hamant and other members of the Candelab, Rebecca Heald (University of California–Berkeley), and Holly Goodson (Notre Dame University) for helpful discussions.

This study was supported by an NIH grant A1054693 to W.Z.C.

REFERENCES

1. **Adam, R. D.** 2001. Biology of *Giardia lamblia*. Clin. Microbiol. Rev. **14:**447–475.
2. **Akhmanova, A., and C. C. Hoogenraad.** 2005. Microtubule plus-end-tracking proteins: mechanisms and functions. Curr. Opin. Cell Biol. **17:**47–54.
3. Reference deleted.
4. **Benchimol, M.** 2004. Participation of the adhesive disc during karyokinesis in *Giardia lamblia*. Biol. Cell **96:**291–301.
5. **Berrueta, L., S. K. Kraeft, J. S. Tirnauer, S. C. Schuyler, L. B. Chen, D. E. Hill, D. Pellman, and B. E. Bierer.** 1998. The adenomatous polyposis colibinding protein EB1 is associated with cytoplasmic and spindle microtubules. Proc. Natl. Acad. Sci. USA **95:**10596–10601.
6. **Best, A. A., H. G. Morrison, A. G. McArthur, M. L. Sogin, and G. J. Olsen.** 2004. Evolution of eukaryotic transcription: insights from the genome of *Giardia lamblia*. Genome Res. **14:**1537–1547.
7. **Blaineau, C., M. Tessier, P. Dubessay, L. Tasse, L. Crobu, M. Pages, and P. Bastien.** 2007. A novel microtubule-depolymerizing kinesin involved in length control of a eukaryotic flagellum. Curr. Biol. **17:**778–782.
8. **Boleti, H., E. Karsenti, and I. Vernos.** 2001. The use of dominant negative mutants to study the function of mitotic motors in the in vitro spindle assembly assay in *Xenopus* egg extracts. Methods Mol. Biol. **164:**173–189.
9. **Briggs, L. J., J. A. Davidge, B. Wickstead, M. L. Ginger, and K. Gull.** 2004. More than one way to build a flagellum: comparative genomics of parasitic protozoa. Curr. Biol. **14:**R611–R612.
10. **Brown, C. L., K. C. Maier, T. Stauber, L. M. Ginkel, L. Wordeman, I. Vernos, and T. A. Schroer.** 2005. Kinesin-2 is a motor for late endosomes and lysosomes. Traffic **6:**1114–1124.
11. **Bu, W., and L. K. Su.** 2001. Regulation of microtubule assembly by human EB1 family proteins. Oncogene **20:**3185–3192.
12. **Campanati, L., A. Holloschi, H. Troster, H. Spring, W. D. Souza, and L. H. Monteiro-Leal.** 2002. Video-microscopy observations of fast dynamic processes in the protozoon *Giardia lamblia*. Cell Motil. Cytoskeleton **51:**213–224.
13. **Cassimeris, L., and C. Spittle.** 2001. Regulation of microtubule-associated proteins. Int. Rev. Cytol. **210:**163–226.
14. **Ciccarelli, F. D., T. Doerks, C. von Mering, C. J. Creevey, B. Snel, and P. Bork.** 2006. Toward automatic reconstruction of a highly resolved tree of life. Science **311:**1283–1287.
15. **Cole, D. G., D. R. Diener, A. L. Himelblau, P. L. Beech, J. C. Fuster, and J. L. Rosenbaum.** 1998. *Chlamydomonas* kinesin-II-dependent intraflagellar transport (IFT): IFT particles contain proteins required for ciliary assembly in *Caenorhabditis elegans* sensory neurons. J. Cell Biol. **141:**993–1008.
16. **Davis-Hayman, S. R., and T. E. Nash.** 2002. Genetic manipulation of *Giardia lamblia*. Mol. Biochem. Parasitol. **122:**1–7.
17. **Dawson, S. C., M. S. Sagolla, and W. Z. Cande.** 2007. The cenH3 histone variant defines centromeres in *Giardia intestinalis*. Chromosoma **116:**175–184.
18. **Deane, J. A., D. G. Cole, E. S. Seeley, D. R. Diener, and J. L. Rosenbaum.** 2001. Localization of intraflagellar transport protein IFT52 identifies basal body transitional fibers as the docking site for IFT particles. Curr. Biol. **11:**1586–1590.
19. **Dentler, W. L.** 1980. Structures linking the tips of ciliary and flagellar microtubules to the membrane. J. Cell Sci. **42:**207–220.
20. **Dentler, W. L., and C. Adams.** 1992. Flagellar microtubule dynamics in *Chlamydomonas*: cytochalasin D induces periods of microtubule shortening and elongation; and colchicine induces disassembly of the distal, but not proximal, half of the flagellum. J. Cell Biol. **117:**1289–1298.
21. **Elmendorf, H. G., S. C. Dawson, and J. M. McCaffery.** 2003. The cytoskeleton of *Giardia lamblia*. Int. J. Parasitol. **33:**3–28.
22. **Filice, F. P.** 1952. Studies on the cytology and life history of a *Giardia* from the laboratory rat. Univ. Calif. Publ. Zool. **57:**53–146.
23. **Gelfand, V. I., N. Le Bot, M. C. Tuma, and I. Vernos.** 2001. A dominant negative approach for functional studies of the kinesin II complex. Methods Mol. Biol. **164:**191–204.
24. **Goshima, G., R. Wollman, N. Stuurman, J. M. Scholey, and R. D. Vale.** 2005. Length control of the metaphase spindle. Curr. Biol. **15:**1979–1988.
25. **Gupta, M. L., Jr., P. Carvalho, D. M. Roof, and D. Pellman.** 2006. Plus end-specific depolymerase activity of Kip3, a kinesin-8 protein, explains its role in positioning the yeast mitotic spindle. Nat. Cell Biol. **8:**913–923.
26. **Hamaguchi, Y., M. Toriyama, H. Sakai, and Y. Hiramoto.** 1987. Redistribution of fluorescently labeled tubulin in the mitotic apparatus of sand dollar eggs and the effects of taxol. Cell Struct. Funct. **12:**43–52.
27. **Hayashi, I., A. Wilde, T. K. Mal, and M. Ikura.** 2005. Structural basis for the activation of microtubule assembly by the EB1 and p150Glued complex. Mol. Cell **19:**449–460.
28. **Helenius, J., G. Brouhard, Y. Kalaidzidis, S. Diez, and J. Howard.** 2006. The depolymerizing kinesin MCAK uses lattice diffusion to rapidly target microtubule ends. Nature **441:**115–119.
29. **Jordan, A., J. A. Hadfield, N. J. Lawrence, and A. T. McGown.** 1998. Tubulin as a target for anticancer drugs: agents which interact with the mitotic spindle. Med. Res. Rev. **18:**259–296.
30. **Kabnick, K. S., and D. A. Peattie.** 1990. In situ analyses reveal that the two nuclei of *Giardia lamblia* are equivalent. J. Cell Sci. **95**(Pt. 3)**:**353–360.
31. **Keister, D. B.** 1983. Axenic culture of *Giardia lamblia* in TYI-S-33 medium supplemented with bile. Trans. R. Soc. Trop. Med. Hyg. **77:**487–488.
32. **Kline-Smith, S. L., A. Khodjakov, P. Hergert, and C. E. Walczak.** 2004. Depletion of centromeric MCAK leads to chromosome congression and segregation defects due to improper kinetochore attachments. Mol. Biol. Cell **15:**1146–1159.
33. **Kline-Smith, S. L., and C. E. Walczak.** 2002. The microtubule-destabilizing kinesin XKCM1 regulates microtubule dynamic instability in cells. Mol. Biol. Cell **13:**2718–2731.
34. **Kozminski, K. G., K. A. Johnson, P. Forscher, and J. L. Rosenbaum.** 1993. A motility in the eukaryotic flagellum unrelated to flagellar beating. Proc. Natl. Acad. Sci. USA **90:**5519–5523.
35. **Ligon, L. A., S. S. Shelly, M. Tokito, and E. L. Holzbaur.** 2003. The microtubule plus-end proteins EB1 and dynactin have differential effects on microtubule polymerization. Mol. Biol. Cell **14:**1405–1417.
36. **Lin-Jones, J., E. Parker, M. Wu, B. E. Knox, and B. Burnside.** 2003. Disruption of kinesin II function using a dominant negative-acting transgene in *Xenopus laevis* rods results in photoreceptor degeneration. Investig. Ophthalmol. Vis. Sci. **44:**3614–3621.
37. **Livak, K. J., and T. D. Schmittgen.** 2001. Analysis of relative gene expression data using real-time quantitative PCR and the $2^{-\Delta\Delta}CT$ Method. Methods **25:**402–408.
38. **Mariante, R. M., R. G. Vancini, A. L. Melo, and M. Benchimol.** 2005. *Giardia lamblia*: evaluation of the in vitro effects of nocodazole and colchicine on trophozoites. Exp. Parasitol. **110:**62–72.
39. **Marshall, W. F., H. Qin, M. Rodrigo Brenni, and J. L. Rosenbaum.** 2005. Flagellar length control system: testing a simple model based on intraflagellar transport and turnover. Mol. Biol. Cell **16:**270–278.
40. **Marshall, W. F., and J. L. Rosenbaum.** 2001. Intraflagellar transport balances continuous turnover of outer doublet microtubules: implications for flagellar length control. J. Cell Biol. **155:**405–414.
41. **Mathur, J., N. Mathur, B. Kernebeck, B. P. Srinivas, and M. Hulskamp.** 2003. A novel localization pattern for an EB1-like protein links microtubule dynamics to endomembrane organization. Curr. Biol. **13:**1991–1997.
42. **Mennella, V., G. C. Rogers, S. L. Rogers, D. W. Buster, R. D. Vale, and D. J. Sharp.** 2005. Functionally distinct kinesin-13 family members cooperate to regulate microtubule dynamics during interphase. Nat. Cell Biol. **7:**235–245.
43. **Mitchison, T., and M. Kirschner.** 1984. Dynamic instability of microtubule growth. Nature **312:**237–242.
44. **Moore, A. T., K. E. Rankin, G. von Dassow, L. Peris, M. Wagenbach, Y. Ovechkina, A. Andrieux, D. Job, and L. Wordeman.** 2005. MCAK associates with the tips of polymerizing microtubules. J. Cell Biol. **169:**391–397.
45. **Moores, C. A., and R. A. Milligan.** 2006. Lucky 13-microtubule depolymerisation by kinesin-13 motors. J. Cell Sci. **119:**3905–3913.
46. **Mueller, J., C. A. Perrone, R. Bower, D. G. Cole, and M. E. Porter.** 2005. The FLA3 KAP subunit is required for localization of kinesin-2 to the site of flagellar assembly and processive anterograde intraflagellar transport. Mol. Biol. Cell **16:**1341–1354.
47. **Nicastro, D., C. Schwartz, J. Pierson, R. Gaudette, M. E. Porter, and J. R. McIntosh.** 2006. The molecular architecture of axonemes revealed by cryoelectron tomography. Science **313:**944–948.
48. **Nohynkova, E., P. Tumova, and J. Kulda.** 2006. Cell division of *Giardia intestinalis*: flagellar developmental cycle involves transformation and exchange of flagella between mastigonts of a diplomonad cell. Eukaryot. Cell **5:**753–761.
49. **Pedersen, L. B., S. Geimer, R. D. Sloboda, and J. L. Rosenbaum.** 2003. The microtubule plus end-tracking protein EB1 is localized to the flagellar tip and basal bodies in *Chlamydomonas reinhardtii*. Curr. Biol. **13:**1969–1974.
50. **Pedersen, L. B., M. S. Miller, S. Geimer, J. M. Leitch, J. L. Rosenbaum, and**

D. G. Cole. 2005. *Chlamydomonas* IFT172 is encoded by FLA11, interacts with CrEB1, and regulates IFT at the flagellar tip. Curr. Biol. **15:**262–266.
51. **Piva, B., and M. Benchimol.** 2004. The median body of *Giardia lamblia*: an ultrastructural study. Biol. Cell **96:**735–746.
52. **Porter, M. E., and W. S. Sale.** 2000. The 9+2 axoneme anchors multiple inner arm dyneins and a network of kinases and phosphatases that control motility. J. Cell Biol. **151:**F37–F42.
53. **Prensier, G., E. Vivier, S. Goldstein, and J. Schrevel.** 1980. Motile flagellum with a "3+0" ultrastructure. Science **207:**1493–1494.
54. **Richardson, D. N., M. P. Simmons, and A. S. Reddy.** 2006. Comprehensive comparative analysis of kinesins in photosynthetic eukaryotes. BMC Genomics **7:**18.
55. **Rogers, G. C., S. L. Rogers, T. A. Schwimmer, S. C. Ems-McClung, C. E. Walczak, R. D. Vale, J. M. Scholey, and D. J. Sharp.** 2004. Two mitotic kinesins cooperate to drive sister chromatid separation during anaphase. Nature **427:**364–370.
56. Reference deleted.
57. **Rosenbaum, J. L., and G. B. Witman.** 2002. Intraflagellar transport. Nat. Rev. Mol. Cell. Biol. **3:**813–825.
58. **Sagolla, M. S., S. C. Dawson, J. J. Mancuso, and W. Z. Cande.** 2006. Three-dimensional analysis of mitosis and cytokinesis in the binucleate parasite *Giardia intestinalis*. J. Cell Sci. **119:**4889–4900.
59. **Savioli, L., H. Smith, and A. Thompson.** 2006. *Giardia* and *Cryptosporidium* join the "Neglected Diseases Initiative". Trends Parasitol. **22:**203–208.
60. **Sawaguchi, A., X. Yao, J. G. Forte, and K. L. McDonald.** 2003. Direct attachment of cell suspensions to high-pressure freezing specimen planchettes. J. Microsc. **212:**13–20.
61. **Scholey, J. M.** 2003. Intraflagellar transport. Annu. Rev. Cell Dev. Biol. **19:**423–443.
62. **Schrevel, J., and C. Besse.** 1975. A functional flagella with a 6+0 pattern. J. Cell Biol. **66:**492–507. (In French.)
63. **Schuyler, S. C., and D. Pellman.** 2001. Search, capture and signal: games microtubules and centrosomes play. J. Cell Sci. **114:**247–255.
64. **Singer, S. M., J. Yee, and T. E. Nash.** 1998. Episomal and integrated maintenance of foreign DNA in *Giardia lamblia*. Mol. Biochem. Parasitol. **92:**59–69.
65. **Sloboda, R. D., and L. Howard.** 2007. Localization of EB1, IFT polypeptides, and kinesin-2 in *Chlamydomonas* flagellar axonemes via immunogold scanning electron microscopy. Cell Motil. Cytoskeleton **64:**446–460.
66. **Smith, E. F., and P. Yang.** 2004. The radial spokes and central apparatus: mechano-chemical transducers that regulate flagellar motility. Cell Motil. Cytoskeleton **57:**8–17.
67. **Snyder, J. A., and J. M. Mullins.** 1993. Analysis of spindle microtubule organization in untreated and taxol-treated PtK1 cells. Cell Biol. Int. **17:**1075–1084.
68. **Sogin, M. L., J. H. Gunderson, H. J. Elwood, R. A. Alonso, and D. A. Peattie.** 1989. Phylogenetic meaning of the kingdom concept: an unusual rRNA from *Giardia lamblia*. Science **243:**75–77.
69. **Solari, A. J., M. I. Rahn, A. Saura, and H. D. Lujan.** 2003. A unique mechanism of nuclear division in *Giardia lamblia* involves components of the ventral disk and the nuclear envelope. Biocell **27:**329–346.
70. **Sun, C. H., and J. H. Tai.** 2000. Development of a tetracycline controlled gene expression system in the parasitic protozoan *Giardia lamblia*. Mol. Biochem. Parasitol. **105:**51–60.
71. **Tan, D., A. B. Asenjo, V. Mennella, D. J. Sharp, and H. Sosa.** 2006. Kinesin-13s form rings around microtubules. J. Cell Biol. **175:**25–31.
72. **Tilney, L. G., and J. R. Gibbins.** 1968. Differential effects of antimitotic agents on the stability and behavior of cytoplasmic and ciliary microtubules. Protoplasma **65:**167–179.
73. **Tirnauer, J. S., J. C. Canman, E. D. Salmon, and T. J. Mitchison.** 2002. EB1 targets to kinetochores with attached, polymerizing microtubules. Mol. Biol. Cell **13:**4308–4316.
74. **Tirnauer, J. S., E. O'Toole, L. Berrueta, B. E. Bierer, and D. Pellman.** 1999. Yeast Bim1p promotes the G1-specific dynamics of microtubules. J. Cell Biol. **145:**993–1007.
75. **Tumova, P., J. Kulda, and E. Nohynkova.** 2007. Cell division of *Giardia intestinalis*: assembly and disassembly of the adhesive disc, and the cytokinesis. Cell Motil. Cytoskeleton **64:**288–298.
76. **Van Damme, D., F. Y. Bouget, K. Van Poucke, D. Inze, and D. Geelen.** 2004. Molecular dissection of plant cytokinesis and phragmoplast structure: a survey of GFP-tagged proteins. Plant J. **40:**386–398.
77. **Varga, V., J. Helenius, K. Tanaka, A. A. Hyman, T. U. Tanaka, and J. Howard.** 2006. Yeast kinesin-8 depolymerizes microtubules in a length-dependent manner. Nat. Cell Biol. **8:**957–962.
78. **Vashishtha, M., Z. Walther, and J. L. Hall.** 1996. The kinesin-homologous protein encoded by the *Chlamydomonas* FLA10 gene is associated with basal bodies and centrioles. J. Cell Sci. **109**(Pt. 3)**:**541–549.
79. **Walczak, C. E., T. J. Mitchison, and A. Desai.** 1996. XKCM1: a *Xenopus* kinesin-related protein that regulates microtubule dynamics during mitotic spindle assembly. Cell **84:**37–47.
80. **Wickstead, B., and K. Gull.** 2006. A "holistic" kinesin phylogeny reveals new kinesin families and predicts protein functions. Mol. Biol. Cell **17:**1734–1743.
81. **Woods, A., T. Sherwin, R. Sasse, T. H. MacRae, A. J. Baines, and K. Gull.** 1989. Definition of individual components within the cytoskeleton of *Trypanosoma brucei* by a library of monoclonal antibodies. J. Cell Sci. **93**(Pt. 3)**:**491–500.